Free Radical Research, February 2008; 42(2): 124–134

informa
healthcare

New method for the detection of reactive oxygen species in anti-tumoural activity of adriamycin: A comparison between hypoxic and normoxic cells

TARECK RHARASS, JEAN VIGO, JEAN-MARIE SALMON, & ANNE-CECILE RIBOU

Institut de Modélisation et d'Analyses en Géo-Environnements et Santé, Université de Perpignan Via Domitia, Perpignan, France

Accepted by Professor M. Davies

(Received 17 July 2007; in revised form 25 November 2007)

Abstract
Tumour hypoxia plays a role in chemoresistance in several human tumours. However, how hyperbaric oxygen leads to chemotherapeutic gain is unclear. This study investigates the relation of reactive oxygen species (ROS) generation with anti-tumoural effect of adriamycin (ADR) on CCRF-CEM cells under hypoxic (2% O_2) and normoxic (21% O_2) conditions. A new method was used to measure intracellular ROS variations through the fluorescence lifetime of 1-pyrenebutyric acid. At 24 h, ADR, probably *via* semiquinone radical, enhances ROS levels in normoxic cells compared to hypoxic cells. Long-term studies show that ROS are also generated by a second mechanism related to cell functions perturbation. ADR arrests the cell cycle progression both under hypoxia and normoxia, indicating that oxygen and ROS does not influence the DNA damaging activity of ADR. The findings reveal that moderate improvement of ADR cytotoxicity results from higher ROS formation in normoxic cells, leading to elevated induction of cell death.

Keywords: *Adriamycin, reactive oxygen species, cell cycle, apoptosis, hypoxia, fluorescence lifetime.*

Introduction

For several decades the anthracycline antibiotic adriamycin (ADR) has been extensively used for clinical treatment of a variety of malignancies. The mechanisms of action of this drug have long been subject to controversy and still remain uncertain. Several mechanisms have been proposed (for review see [1,2]) and for many years the cytotoxicity of ADR was explained by its intercalation into DNA between adjacent base pairs and the subsequent inhibition of DNA replication [3]. Other modes of action have been proposed to explain ADR cytotoxicity. Amongst them, it was established that anthracyclines induce an increase of reactive oxygen species (ROS) formation. ADR can accept electrons from oxoreductive enzymes in the mitochondria to form semiquinone free radicals, which can reduce molecular oxygen to oxygen radicals [4–6].

The presence of oxygen seems essential for the efficiency of ADR. Indeed, several studies reported that hypoxic condition of tumours induced resistance to ADR in various cell lines *in vitro* and *in vivo*, while chemosensitivity to the agent increased in oxygenated cells [7–9]. Hypoxia is a common feature of many tumours, occuring as a result of an inadequate delivery of oxygen due to an exponential proliferation of cancerous cells and an insufficient vascular supply [10]. Many studies have been conducted to investigate possible adjunctive therapy leading to therapeutic

Correspondence: Anne-Cecile Ribou, Institut de Modélisation et d'Analyse en Géo-Environnements et Santé, IMAGES, EA4218, Université de Perpignan Via Domitia, 52 av. Paul Alduy, 66860, Perpignan, France. Tel: +1 (33) 468 662 113. Fax: +1 (33) 468 662 144. Email: ribou@univ-perp.fr

ISSN 1071-5762 print/ISSN 1029-2470 online
DOI: 10.1080/10715760701834552

gain. Hyperbaric oxygen (HBO) is widely used as adjunctive therapy in several clinical indications including treatment of non-healing wounds. HBO increases the amount of dissolved oxygen in the blood and therefore can lead to an increase of the oxygen availability within tumours. It has been shown that HBO affects growth of tumour cells and improves chemotherapy and radiotherapy. In particular, it has been reported that HBO enhanced the cytotoxic activity of ADR [11,12]. However, the mechanisms leading to the improvement of chemotherapeutic efficacy of the drug are not well understood.

We propose to investigate the effect of the variation of cell oxygenation on ROS production due to ADR treatment. We developed a new method in our laboratory consisting in measurement of 1-pyrenebutyric acid (PBA) fluorescence lifetime by time-resolved microfluorimetry. The main advantage of this method is that fluorescence lifetime measurements are independent of the absolute intensity of the emitted light and, therefore, independent of the intracellular accumulation of the probe. Thus, the method is less prone to errors and shows good sensitivity compared with other methods that use fluorescence intensity. PBA is a fluorescent probe with a long fluorescence lifetime depending on the concentration of molecular oxygen, but also on the intracellular level of ROS [13]. Fluorescence lifetime measurements of PBA in cells had permitted an evaluation of the ROS variations under various conditions [14].

It is important to monitor the effect of ADR treatment on the cell proliferation. Fluorescence image analysis by videomicrofluorimetry is a complementary method to flow cytometry to analyse dynamic events in cell populations. We developed a triple labelling method to study living cell populations under different conditions and for different cell lines [15,16]. Cells were simultaneously labelled with fluorescent probes (Hoechst 33342, Rhodamine 123 and Nile Red) which, respectively, stain nuclei, mitochondria and plasma membranes. Image digitization allowed us to collect several parameters computed in a multiparametric approach to study relations between morphological parameters (size, shape) and functional parameters (membrane properties, mitochondrial energetic state, DNA synthesis). This is particularly useful for the study of the cell cycle distribution [17].

In this paper, we quantified ROS fluctuations and studied distribution into the cell cycle phases in cultured CCRF-CEM cancerous cell line incubated under hypoxic (2% O_2) or normoxic (21% O_2) conditions with 1.7 μM of ADR. In parallel, the effects of the anthracycline on cell proliferation and viability were compared between the two conditions of oxygenation. The data on mitochondrial energetic state and DNA content have allowed us to identify and quantify apoptotic cells. These modifications of treated cells were followed daily during 6 days.

Materials and methods

Chemicals

Cell culture medium RPMI 1640, Hanks' balanced salt solution (HBSS), penicillin and streptomycin antibiotics, foetal bovine serum and L-glutamine were provided by Cambrex (Verviers, Belgium). Adriamycin (ADR) (Sigma, St. Quentin Fallavier, France) was prepared in phosphate-buffered saline (PBS) solution (ICN Biomedicals, Costa Mesa, CA) to 0.5 mM and stored at -20°C. Stock solutions of Hoechst 33342 (Ho342) (Aldrich, St. Quentin Fallavier, France) and Rhodamine 123 (R123) (Sigma, St. Quentin Fallavier, France) were prepared in PBS to 1 mM and 0.1 mM, respectively, and stored at -20°C. Nile Red (NR) was provided by Sigma (St. Quentin Fallavier, France), prepared in ethanol (95%) to 1 mM and stored at 4°C. 1-pyrenebutyric acid (PBA) was purchased from Acros Organics (Geel, Belgium), dissolved in ethanol (95%) to 50 μM and stored at 4°C.

Cell culture and treatment

Human lymphoblastic cells CCRF-CEM provided by Dr W. T. Beck (College of Medicine, University of Illinois at Chicago, Chicago, IL) were grown as stationary suspension cultures in RPMI 1640 medium supplemented with 2 mM L-Glutamine, 10% heat-inactivated foetal bovine serum and 1% of antibiotics at 37°C in a humidified incubator containing 21% O_2, 5% CO_2 in air (referred to hyperoxygenated condition compared to hypoxic tumour level). The cells were seeded every 3 or 4 days at 0.2×10^6 cells/ml to maintain exponential growth. Appropriate volume of ADR was added into 5 ml complete medium containing 0.2×10^6 cells/ml, to reach a final drug concentration of 1.7 μM (1000 ng/ml). To simulate hypoxic tumour conditions, cells were immediately placed after drug addition in a humidified incubator chamber equiped with a flowmeter (Aalborg, NY) allowing us to flush the cells with a gas mixture of 2% O_2, 93% N_2 and 5% CO_2 during 2 h. The flows were regulated at 10, 465 and 25 ml/min, respectively. The chamber was sealed and adjusted at 37°C. The flushing procedure was repeated each day for 2 h to maintain a constant atmosphere into the chamber. A pressure of 1 atm was kept constant during the experiments. Cells were Coulter-counted (model ZM, Beckman Coulter, Paris, France) each 24 h to evaluate the cell growth. Two replicates of each condition were used in each assay. Cell counts were performed in triplicate. Cell viability was evaluated by trypan blue exclusion assay.

Each condition was asseyed in duplicate. Experiments were performed twice.

Staining procedure

For time-resolved microfluorimetry experiments, the cell suspension containing 0.6×10^6 cells was incubated for 20 min in 900 µl HBSS with 10.8 µl of PBA (0.6 µM, final concentration), at 37°C. The cells were centrifuged and rinsed twice. They were finally resuspended in 900 µl HBSS and 300 µl of the solution (i.e. 0.2×10^6 cells) was placed on a Sykes-Moore chamber for measurements of PBA fluorescence lifetimes. Each experiment was performed daily during 6 days and repeated three times.

For numerical analysis experiments, cell sample was prepared by adding 10 µl of Ho342 (10^{-5} M, final concentration) to 1 ml of cell suspension containing 1.0×10^6 cells. After 1 h of incubation, 115 µl of R123 (10^{-5} M, final concentration) was added to the cell suspension. The cells were further incubated for 57 min with the two probes before 17 µl of NR (1.5×10^{-5} M, final concentration) was added. After 3 min, the cells were centrifuged and rinsed three times. They were suspended in 1 ml HBSS and an aliquot of the cell suspension (300 µl) was removed and plated in a Sykes-Moore chamber for numerical image analysis. These analyses were performed after 2 h, 6 h, 18 h and each 24 h during 6 days and repeated 2–3 times.

Numerical image acquisition and analysis

The fluorescence digital imaging microscopy system has been described elsewhere in detail [17,18]. For each experiment, 22 parameters were evaluated, including cell and nucleus areas and perimeters, shape factors for cell and nucleus and fluorescence intensity parameters (total, mean and standard error) for Ho342, R123 and NR on $\sim$ 600 cells. The fluorescence intensity parameters were normalized using a reference standard to compensate for intensity fluctuations of the mercury lamp. The sizes and shape factors of cells and nuclei were used to exclude cell clumps and debris and to keep only isolated cells. The total fluorescence intensities of Ho342, R123 and NR were analysed to monitor variations of morphological and functional properties of each cell. A set of seven parameters (cell and nucleus area and perimeter, total fluorescence intensity and associated mean and standard deviation of Ho342) were selected and used in a multiparametric approach for cell cycle classification. The multiparametric data analysis ran with XLSTAT-Pro software (Addinsoft, Paris, France) and consisted of typology (agglomerative hierarchical clustering and k-means clustering) followed by discriminant analysis [17].

Fluorescence decay recording and analysis

The apparatus has been previously described in detail [14,19]. PBA-loaded single cells were excited at a wavelength of 337 nm with a nitrogen laser. The pyrene emission was selected by a 404 nm interference filter. We obtained a biexponential decay: the first decay corresponded to the intrinsic fluorescence of the cell (i.e. NAD(P)H fluorescence) and the second decay was a longer one corresponding to the PBA fluorescence. The substraction of this biexponential decay with a decay curve resulting from a cell without probe loading (i.e. intrinsic fluorescence of the cell) allowed us to obtain a decay curve of PBA alone and to eliminate the baseline response of the detector. The resulting decay was simulated with a single exponential decay using the downhill simplex method [20] to obtain values of PBA fluorescence lifetimes. Fluorescence lifetime measurements were achieved under (i) air and (ii) nitrogen atmospheres. Diminishing the oxygen concentration in the cell atmosphere was performed using a flowmeter supplying N_2 gas [14] to simplify the deactivation processes of PBA fluorescence. Stable PBA fluorescence lifetimes were usually obtained after 10 min (residual oxygen concentration lower than 0.5% [19]). The measurements were achieved between 21–24°C. During the period of experimentation (< 30 min), no significant fluctuations of NAD(P)H fluorescence intensities (i.e. energetic state of the cells) were detected neither for measurements performed under air atmosphere nor for those under nitrogen atmosphere. We tested several cells in each sample and we did not detect any time-dependent changes. These results confirm that cells remained physiologically intact and that ROS formation was stable during the experiments.

Stern-Volmer analysis of quenching

To calculate the ROS variations from experimental data (i.e. fluorescence lifetimes), we used the Stern-Volmer equation (Equation 1) as shown below. In the absence of static quenching, collisional fluorescence quenching by molecular oxygen is described by the Stern-Volmer equation 21:

$$\tau_0/\tau = 1 + k_q \tau_0 [Q] \quad (1)$$

In this equation, τ_0 and τ are the PBA fluorescence lifetimes in absence and presence of quencher, respectively, k_q is the quencher quenching rate constant and [Q] is the quencher concentration. In a complex cellular environment, oxygen but also several ROS can deactivate PBA fluorescence [13,14]. If we make the simple assumption of two independent quenchers, we obtain the intracellular total ROS variation by comparing two treatment conditions [14]:

$$\frac{[ROS]_{treatment}}{[ROS]_{control}} = \frac{(\tau_0 - \tau_{treatment}) \times \tau_{control})}{(\tau_0 - \tau_{control}) \times \tau_{treatment})} \quad (2)$$

where $[ROS]_{treatment}$ and $[ROS]_{control}$ are the reactive oxygen species concentrations in treated cells and control cells, respectively. τ_0 is the PBA fluorescence lifetime in absence of O_2 and ROS. It was measured under nitrogen atmosphere (oxygen highly reduced) on cells fixed with Baker solution (10% paraformaldehyde in 1% aqueous calcium chloride). After fixation, we assumed that cell activity was blocked and ROS production was stopped [14]. Similar τ_0 values were obtained whatever the cell treatment used (average: 209 ns) consistent with the total removal of ROS. The fluorescence lifetimes $\tau_{control}$ (average: 197 ns) and $\tau_{treatment}$ were measured under nitrogen atmosphere on control and treated cells, respectively. We have assigned an arbitrary value of 1 to the ROS concentration of control cells. This allowed us to give arbitrary values for ROS concentrations.

Results

Reactive oxygen species generation

The anti-cancerous agent ADR is described to generate ROS [1,2,5,6]. To monitor ROS fluctuations, we recorded the fluorescence lifetimes of the probe 1-pyrenebutyric acid (PBA) on cells loaded with PBA, using time-resolved microfluorimetry. This method was recently developed for measurements in living cells [14]. Cells were treated with ADR at the dose of 1.7 μM and incubated either under simulated hypoxic or normoxic condition during 144 h. Figure 1A shows the means of the PBA fluorescence lifetimes obtained from the measurements performed under air atmosphere. To simplify the deactivation processes of the probe and to obtain one equation allowing us to calculate the variations of intracellular ROS levels, we also performed the measurements under nitrogen atmosphere. In Figure 1B, we present the variations of ROS concentrations obtained after calculation using Equation (2). For control, no significant PBA fluorescence lifetime variations were observed between hypoxic cells and normoxic cells (Figure 1A). The means of fluorescence lifetimes remained constant throughout the experiments (~160 ns). The measurements performed with control cell populations showed standard deviations (SD) of ~4 ns. This value is consistent with a homogeneous population. For cells treated with ADR 1.7 μM then incubated under hypoxic condition, PBA fluorescence lifetimes slightly changed at 24 h (mean: 157 ns). This corresponded to a weak increase of intracellular ROS quantities (mean: 1.25 a.u. compared to 1.05 a.u. for control cells). Then, the decrease of the fluorescence lifetimes continued corresponding to a progressive increase of the ROS production. We obtained 153 ns at 72 h (ROS: 1.5 a.u.) and we reached a mean value of 150 ns (1.85 a.u.) after 144 h of treatment under hypoxia. SD values increased with time (3 ns at 24 h compared to 8 ns at 144 h), indicating that cell population presented an important dispersion of ROS values. Indeed, some treated cells still exhibited ROS levels close to those obtained for control cells. Under normoxic condition, the generation of ROS by ADR was greatly enhanced. We observed an earlier and higher reduction of PBA fluorescence lifetimes (149 ns at 24 h) corresponding to a ROS concentration of 2.1 a.u. (Figure 1B). We had previously observed similar reduction of PBA fluorescence lifetimes already at 4 h, in the same conditions of cell treatment [13]. Then, the means and SD remained stables during the 144 h of treatment (mean: ~148 ns; SD: ~4 ns), corresponding to ROS quantities two-fold the control value.

Cell growth and viability

In order to examine the influence of ADR on cell proliferation, cell density was evaluated by Coulter-counter each 24 h during 144 h. The cell viability was assayed by trypan blue exclusion. CCRF-CEM cells were seeded in complete culture medium at an initial cell density of 0.2×10^6 cells/ml and then incubated under two different oxygen levels. Figure 2 shows a similar cell growth for control cells incubated under hypoxia (2% O_2) and normoxic condition (21% O_2). The cell density increased during the first 96 h (1.7×10^6 cells/ml and 1.8×10^6 cells/ml under 2% and 21% O_2, respectively) and the number of non-viable cells did not exceed 4% (Table I). The cell growth was stopped after 96 h. A stationary phase (i.e. plateau) was reached, certainly due to the impoverishment of the culture medium, and we observed an increase of the number of non-viable cells (~ 12% at 144 h). For these reasons, fluorescence lifetime measurements and cell cycle analysis were not performed on control cells after 96 h of incubation. Treatment with ADR 1.7 μM led to an immediate stopping of the cell growth both under 2% and 21% O_2. The Coulter-counting of the number of cells remained stable during the 144 h of treatment (0.2×10^6 cells/ml). Moreover, ADR induced a time-dependent decrease in cell viability under the two oxygen concentrations (Table I). After 144 h of treatment, we obtained 56% of non-viable cells under 21% O_2 compared with 40% under hypoxia.

Apoptosis detection

Cell staining with Rhodamine 123 (R123) and Hoechst 33342 (Ho342) permits us to determine the mitochondrial energetic state of the cells and the DNA content, respectively. Indeed, R123 has been widely used to evaluate the mitochondrial membrane potential in various cells [22,23] and Ho342

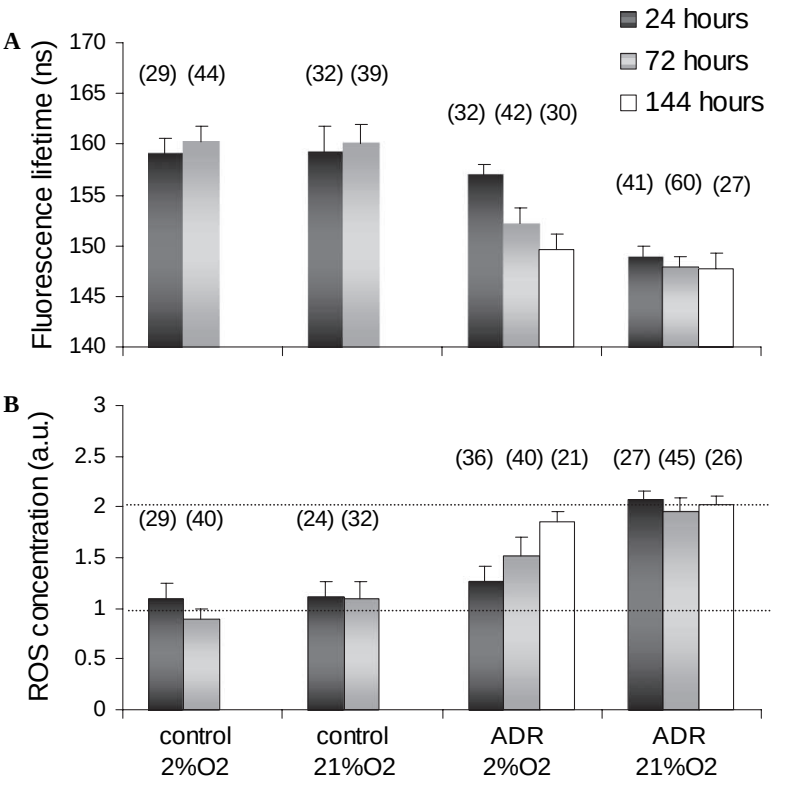

Figure 1. PBA fluorescence lifetimes (A) and ROS concentrations (B) for control cells and cells treated with ADR 1.7 μM then incubated under 2% or 21% O_2. Measurements were performed each 24 h, we only show data recorded for 24, 72 and 144 h. The values were measured (A) under air atmosphere and (B) under nitrogen atmosphere (highly reduced oxygen flow). Values are means ± SEM (standard error of the mean) of three independent experiments. The number of cells (*n*) is indicated in each case.

fluorochrome binds to A-T rich sites in the DNA minor groove and covers four base pairs, AATT [24]. These two parameters should allow us to discriminate apoptotic cells. Indeed, the loss of mitochondrial membrane potential is considered as an early indicator for commitment of cells into programmed cell death [22,25]. Moreover, cells entered in apoptotic death can be recognized by their diminished stainability with DNA-binding dye due to alteration and subsequent loss of chromatin. We monitored the ratio of the total fluorescence intensity of R123 to the cell volume (tFI_{R123}/V_{cell}), which indicates the mitochondria energetic state of the cells regardless of the possible increase of the cell sizes, vs the total fluorescence intensity of Ho342 (tFI_{Ho342}), as illustrated in Figure 3. The data presented in this figure correspond to control and ADR-treated cells (1.7 μM) incubated 72 h under 21% O_2. Especially for cells treated with ADR, a sub-population differed from the cellular pool and presented tFI_{R123}/V_{cell} ratio values significantly smaller than 0.2 (mean: 0.04 compared to 0.51 and 0.46 for the pools of ADR-treated and control cells, respectively), indicating a decrease of the mitochondrial energetic state. This sub-population represented less than 3% of the total population for control while it corresponded to 14% for ADR-treated cells at 72 h (Table I). The majority of the cells with low tFI_{R123}/V_{cell} ratio exhibited at the same time a considerable decrease of tFI_{Ho342}, i.e. reduction of DNA content (mean: 7500 a.u. compared to 15 000 a.u. for G_0/G_1 group, for ADR-treated cells at 72 h (Table II)). The tFI_{Ho342} values continued to decrease throughout time of treatment (mean: 3500 a.u. for the sub-population at 144 h). Moreover, this sub-population presented a nuclear condensation (average value of nucleus area: 243 a.u. compared with 380 a.u. for G_0/G_1 group) consistent with apoptotic processes [26]. Since cells were also stained with Nile Red as described in the Materials

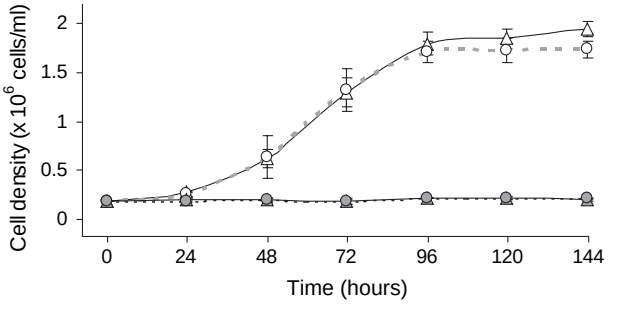

Figure 2. Effects of ADR treatment (1.7 μM) on CCRF-CEM cell growth. Cells were incubated at 0.2×10^6 cells/ml with the drug for 144 h. Every 24 h, aliquots of the cell suspensions were removed and cells counted using a Coulter-counter. Control 2% O_2 (○), control 21% O_2 (△), ADR 2% O_2 (●) and ADR 21% O_2 (▲). Results are given as means ± SD of 3–4 independent experiments performed in duplicate.

Table I. Proportion of apoptotic cells (i.e. $tFIR_{123}/V_{cell} < 0.2$) and non-viable cells (i.e. trypan blue-stained cells) obtained for control cells and ADR-treated cells (1.7 μM). Cells were incubated under hypoxic (2% O_2) or normoxic (21% O_2) conditions during treatment. Measurements were performed several times (see Materials and methods), some of them are shown here.

	Control cells						Adriamycin 1.7 μM												
	2% O_2		21% O_2				2% O_2						21% O_2						
	18 h	72 h	2 h	6 h	18 h	72 h	6 h	18 h	24 h	48 h	72 h	144 h	2 h	6 h	18 h	24 h	48 h	72 h	144 h
Apoptosis* (%)	2	2	2	1	3	3	2	4	6	8	8	19	2	2	3	5	10	14	30
Non-viable cells (%)	4	3	3	3	4	3	3	6	6	11	20	40	3	3	6	7	15	27	56

* obtained from videomicrofluorimetry experiments.

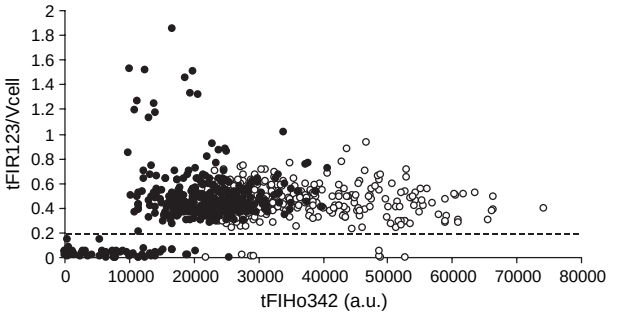

Figure 3. Ratio of the total fluorescence intensity of Rhodamine 123 to the cell volume (tFI_{R123}/V_{cell}) vs the total fluorescence intensity of Hoechst 33342 (tFI_{Ho342}). Measurements were obtained in control cells (hollow symbols) and cells treated with ADR 1.7 μM (full symbols). Cells were incubated under 21% O_2 during 72 h.

and methods section, we observed that plasma membranes of the sub-population were still intact. Indeed, cells entering into apoptosis present no disruption of the plasma membranes, while necrosis is accompanied by a rapid plasma membrane permeabilization leading to efflux of cell constituents in extracellular space [27]. The percentage of apoptotic cells (Table I) was determined from the number of cells in the sub-population characterized by tFI_{R123}/V_{cell} ratio values < 0.2. We compared control and ADR-treated cells (1.7 μM) incubated under hypoxic (2% O_2) or normoxic (21% O_2) conditions during 144 h. For both controls, the percentage of apoptotic cells remained stable throughout the time-period of the experiments ($\sim 3\%$ of the total cell populations). Treatment with ADR induced an increase of the number of apoptotic cells which became moderately higher under normoxia compared with hypoxia after 48 h. We obtained at 144 h 30% of apoptotic cells under 21% O_2 compared to 19% under hypoxia. To prevent erroneous classification of apoptotic cells in the different phases of the cell cycle as viable cells, we pulled off the distinct sub-population presenting tFI_{R123}/V_{cell} ratio values < 0.2 (Figure 3) from the initial cell population before using the multiparametric analysis for cell cycle distribution. The arbitrary ratio value of 0.2 remained the same whatever the cell population or the time treatment and clearly delimited the sub-population from the rest of the cell population.

Cell cycle analysis and DNA alteration

We investigated the effects of ADR (1.7 μM) on cell progression through the cell cycle under hypoxic and normoxic conditions. Figure 4 shows the percentage of cells obtained for different phases of the cell cycle. Cells were classified in three groups related to diploid cell cycle phases (G_0/G_1, S, G_2+M) and two groups of polyploid cells (Gn_1 and Gn_2). We observed that the ratio of G_2+M group to G_0/G_1 group for DNA labelling was close to 2 ($\pm 5\%$) in all cases (Table II). Control cells incubated under hypoxia presented comparable cell cycle distribution to control cells incubated under 21% O_2 (Figure 4). Since we seeded CCRF-CEM cells in fresh cell culture medium every 3 days, the distribution of the cell cycle at the very beginning of incubation (i.e. 2 h) and at 72 h were equivalent ($\sim 50\%$ of cells in G_0/G_1 group). After 6 h, control cells accumulated in the S-phase ($\sim 40\%$ vs $\sim 25\%$ at initial time) due to an increase of G_0/G_1–S transition. On the contrary, the cell cycle distribution remained unchanged between 2–6 h of treatment with ADR when incubated both under 2% and 21% oxygen (Figure 4). Apparently, ADR delayed the rate of traversal from G_0/G_1 to S phase. After 18 h of drug treatment, we observed a decrease of the number of cells in G_0/G_1 group both under hypoxia and normoxic condition. The percentage of cells in S and G_2+M phases increased ($\sim$ 40% and $\sim$ 30%, respectively). The reduction of the G_0/G_1 group was due to the cell progression through S-phase and subsequently through G_2+M group. Moreover, since ADR stopped the cell proliferation at the dose selected (Figure 2), this implies a cell blocking in

Table II. Means of the total fluorescence intensity of Ho342 ($mtFI_{Ho342}$) for each phase of the cell cycle. Cell populations are the same as those presented in Figure 4. Results are given as means in arbitrary units. Some data on apoptotic population and data on Gn_2 phase are not presented due to the scarcity or absence of cells.

			Phases of the cell cycle (a.u.)				
	Time (h)	Number of cells	G_0/G_1	S	G_2+M	Gn_1	Apoptosis (a.u.)
Control 2%O_2	72	1004	25 000	35 000	48 000	61 000	—
Control 21%O_2	72	803	26 000	37 500	50 000	63 500	—
ADR 2%O_2	6	564	20 000	28 000	38 500	47 500	—
	18	481	14 000	21 000	28 000	36 500	—
	72	914	15 500	25 000	32 000	41 000	8000
ADR 21%O_2	2	498	25 500	36 500	52 500	73 000	—
	6	523	18 500	26 000	35 000	44 000	—
	18	548	14 500	20 000	30 000	39 000	—
	72	926	15 000	21 500	29 000	39 000	7500
	144	835	14 700	22 000	29 500	38 500	3500

the G_2+M group, preventing the renewal of cells in G_0/G_1. This cell-cycle distribution remained unchanged until 144 h (Figure 4) and this whatever the oxygen level used during incubation.

Since adriamycin [1,2] and Hoechst 33342 [24] are both DNA-binding molecules, the staining of the nuclei with Ho342 intercalating dye can be affected by previous cell treatment with ADR. Monitoring the resulting decrease in Ho342 fluorescence intensity can supply informations about the DNA-binding of ADR at the dose of 1.7 μM and subsequent DNA alteration. Table II shows the means of the total fluorescence intensities of Ho342 ($mtFI_{Ho342}$) obtained for different phases of the cell cycle. Control cells presented similar $mtFI_{Ho342}$ values both under hypoxic and normoxic conditions. These values remained stable throughout the experiments. Cells treated 2 h with ADR showed comparable $mtFI_{Ho342}$ values to control values, both under 2% O_2 and 21% O_2. The $mtFI_{Ho342}$ values decreased by $\sim$ 20% at 6 h and continued to decrease at 18 h ($\sim$ 40%). Afterwards $mtFI_{Ho342}$ values remained stables. The observed decrease in $mtFI_{Ho342}$ affected in the same way the cells incubated under 2% or 21% of oxygen for the first 72 h.

Discussion

The aim of this study consists of investigating the link between reactive oxygen species (ROS) generation and cytotoxic/cytostatic activity due to the chemotherapeutic agent adriamycin (ADR). The treated cells were incubated under simulated hypoxic tumour condition (2% O_2) and under normoxia (21% O_2, regarded as hyperoxygenated physiological condition in tissues). We compared the efficiency of anticancerous effect of ADR between the two oxygenation conditions. First, we observed that untreated CCRF-CEM cells normally proliferated under hypoxia since neither the cell growth (Figure 2) nor the cell death (Table I) were affected after decreasing the exogenous oxygen delivery compared to normoxic condition. This is consistent with the analysis of the cell cycle distribution showing similar classification between untreated hypoxic and normoxic cells (Figure 4). We did not measure significant variations of ROS concentrations in untreated CCRF-CEM cell line, even if either an increase [28,29] or a decrease [30,31] in the ROS production during hypoxia was already reported in the literature for other cultured cells. Our results suggest that under 2% of oxygen, CCRF-CEM cells have at their disposal enough oxygen to continue generating the same quantity of ROS as normoxic cells and that oxygen is not a limiting factor to this production.

It is widely accepted that ADR generates ROS [1,2,4–6]. This generation is partly due to the quinone structure of ADR which can be reductively activated to semiquinone free radical intermediate in the mitochondria. The semiquinone free radical can react with O_2 which is converted to superoxide anion, leading to an increase of intracellular ROS production. Our experiments show that cultivating the ADR-treated cells (1.7 μM) under normoxic condition

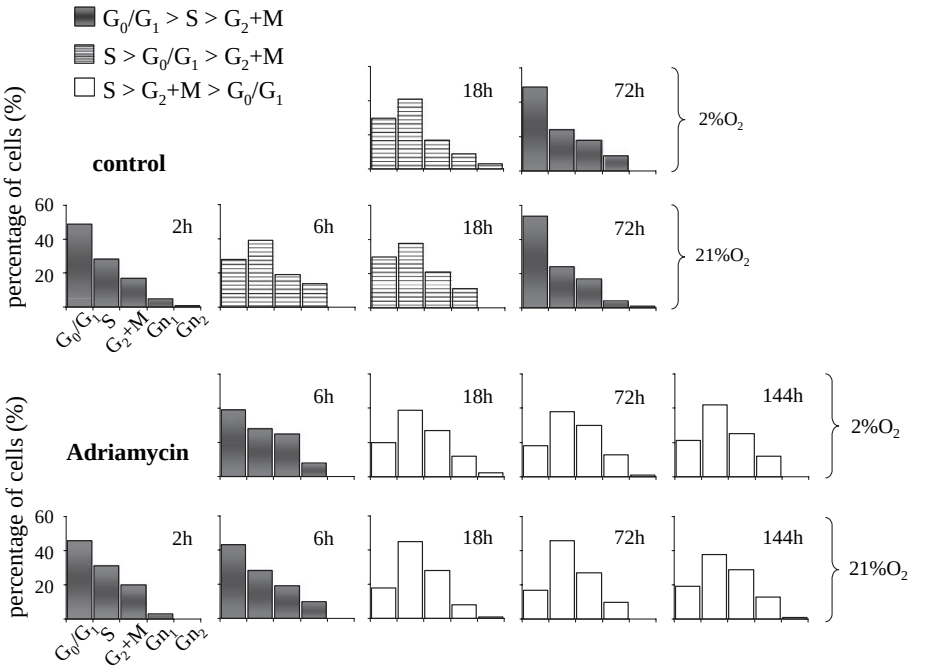

Figure 4. Proportion of cells in the different phases of the cell cycle (G_0/G_1, S, G_2+M, Gn_1 and Gn_2). Cells were treated or not with ADR 1.7 μM and incubated under hypoxic (2% O_2) or normoxic (21% O_2) conditions. We monitored cell-cycle distribution for various times as explained in the Materials and methods section. We present selected data (2, 6, 18, 72 and 144 h of incubation). The percentages are calculated from the number of cells with $tFI_{R123}/V_{cell} > 0.2$.

favours ROS generation compared to hypoxia. Indeed, for treated cells incubated 24 h under 2% O_2, the increase of ROS production did not exceed 20%, whereas ROS level increased two-fold for treated cells cultivated under 21% O_2. For longer time, ROS production due to one-electron redox cycling of the drug (i.e. direct effect) decreases and even stops after metabolization of ADR. Thus, the observation of a stable ROS production under 21% O_2 and an increase under 2% O_2 after several days (Figure 1) cannot be due to direct effect of ADR. This is consistent with the proposal of two mechanisms reported in the literature [1,2]. They suggest that ROS may not only be generated in response to direct effect of ADR but also in response to delayed perturbation of cell metabolism and function resulting from the treatment. Other argument in favour of a second mechanism is that after 6 days of treatment, the cells incubated under hypoxia showed ROS concentrations with high standard deviation. Some of the values were similar to those obtained in treated cells incubated under 21% O_2, others were close to ROS levels in untreated cells. Here again, these differences are unlikely to result from the direct effect of ADR. Further experiments are necessary to elucidate the mechanisms leading to the substantial delay of ROS generation occurring in ADR-treated cells under hypoxic condition. However, we can conclude that ROS generation by the antibiotic drug ADR at 1.7 μM is promoted when treated cells are incubated under normoxic conditions compared to hypoxic level both *via* direct mechanism and cell functions perturbation.

We showed in Figure 2 that ADR at the dose selected (1.7 μM) immediately stopped the cell growth both under hypoxic and normoxic conditions. This is consistent with results obtained with the analysis of the cell cycle distribution presented in Figure 4. Our data are similar to the results reported in the literature under normoxia, for different cell lines but with similar drug level [32,33]. During the first hours, ADR treatment led to a delay of the G_0/G_1–S traverse compared to control. Then, ADR-treated cells accumulated in S and G_2+M phases and finally the cell cycle was completely stopped. Here we showed that cell cycle distribution was similar when treated cells were incubated under hypoxic conditions. Therefore, changing the oxygen level, and consequently the ROS production, did not modify ADR effect on the cell cycle. On top of information on the cell-cycle distribution, videomicrofluorimetry studies allowed to quantify Ho342 that binds to the nuclei by direct measure of the total fluorescence intensity of the dye (tFI_{Ho342}). We can question if the binding of ADR to DNA can exclude the subsequent binding of Ho342. However, after 2 h, tFI_{Ho342} were similar in treated and control cells. Since the uptake of ADR is fast (~ 60 min) [34], it seems unlikely that the two molecules would compete for the same binding sites. It is more probable that we indirectly evaluated the DNA alteration resulting from the drug treatment. Later, we observed (Table II) that the treatment led to a considerable decrease of tFI_{Ho342} compared to control cells. This decrease occurred at the same level both under hypoxic and normoxic conditions. The maximum decrease of tFI_{Ho342} was reached at 18 h. Similarly, we had to wait 18 h to obtain a complete blocking of the cell cycle distribution. At this point, we confirm the connection between the DNA alteration and the progression through the cell cycle. When tFI_{Ho342} becomes constant, there is no more progression through the cell cycle. Several authors proposed that those DNA alterations were due to alkylation of DNA. The ADR-DNA adducts were described and characterized [35]. Moreover, we suppose that ROS production was not involved in cell cycle blocking since the exogenous oxygen level used during incubation of ADR-treated cells affected the ROS production but not the cell cycle distribution. Thus, the anti-proliferative effect of ADR, resulting in the cell cycle blocking, seems mainly due to the interference of the antibiotic drug with cellular DNA rather than a change in the ROS production.

We investigated the effect of oxygen level changes on cytotoxic effect of ADR through measurement of cell viability using trypan blue exclusion assay. As expected, ADR treatment led to a decrease of cell viability as shown in Table I. The number of non-viable cells was higher under normoxic condition than under hypoxic condition. We also monitored the amount of apoptotic cells since it has been reported that apoptosis induction is involved in the cytotoxic activity of ADR at pharmacologically relevant concentrations [36–38]. We identified apoptotic cells by a substantial drop of the mitochondrial energetic state (i.e. tFI_{R123}/V_{cell} ratio) and a decrease of DNA content resulting in high reduction of tFI_{Ho342}. A significant increase of the number of apoptotic cells followed ADR treatment. The apoptosis phenomenon occurred equally in all the phases of the cell cycle since the cell classification remained unchanged. Even if modifying the oxygen level induced no change for untreated cells, we observed after treatment a greater increase of the quantity of apoptotic cells under normoxic conditions. These results are coherent with the variation of ROS concentrations. Under hypoxia, we observed a delayed ROS generation compared with normoxic cells in which a high intracellular ROS level is reached earlier. Indeed, it has been reported that ROS can serve as an intracellular signal in the apoptotic pathway [39,40]. Our results imply that the lower amount of apoptotic cells observed after ADR treatment under hypoxia is due to the lower ROS concentration and not to a change of the nuclear.

In this paper, we show that efficiency of the chemotherapeutic agent adriamycin is higher in normoxic cells compared to hypoxic cells. This confirms observations reported by other groups [7–9]. We suggest that improvement of the cytotoxic activity of ADR at the clinically relevant level of 1.7 μM likely results from higher intracellular ROS generation in normoxic cells, leading to a greater induction of apoptotic cell death. However, the oxygen level seems to have no effect on the cell cycle arrest. We are currently investigating the effects of lower ADR concentrations on these mechanisms.

Acknowledgements

This work was supported by grants from the French 'Ligue Nationale Contre le Cancer' Comités des Pyrénées-Orientales et du Gard. The authors are grateful to Dr Julien Savatier for helpful suggestions and critical reading of the manuscript.

References

[1] Gewirtz DA. A critical evaluation of the mechanisms of action proposed for the antitumor effects of the anthracycline antibiotics adriamycin and daunorubicin. Biochem Pharmacol 1999;57:727–741.

[2] Minotti G, Menna P, Salvatorelli E, Cairo G, Gianni L. Anthracyclines: molecular advances and pharmacologic developments in antitumor activity and cardiotoxicity. Pharmacol Rev 2004;56:185–229.

[3] Cullinane C, Cutts SM, van Rosmalen A, Phillips DR. Formation of adriamycin-DNA adducts *in vitro*. Nucleic Acids Res 1994;22:2296–2303.

[4] Davies KJA, Doroshow JH. Redox cycling of anthracyclines by cardiac mitochondria. I. Anthracycline radical formation by NADH dehydrogenase. J Biol Chem 1986;261:3060–3067.

[5] Doroshow JH, Davies KJA. Redox cycling of anthracyclines by cardiac mitochondria. II. Formation of superoxide anion, hydrogen peroxide and hydroxyl radical. J Biol Chem 1986;261:3068–3074.

[6] Quiles JL, Huertas JR, Battino M, Mataix J, Ramirez-Tortosa MC. Antioxidant nutrients and adriamycin toxicity. Toxicology 2002;180:79–95.

[7] Teicher BA, Holden SA, Al-Achi A, Herman TS. Classification of antineoplastic treatments by their differential toxicity toward putative oxygenated and hypoxic tumor subpopulations *in vivo* in the FSaIIC murine fibrosarcoma. Cancer Res 1990;50:3339–3344.

[8] Frederiksen LJ, Siemens DR, Heaton JP, Maxwell LR, Adams MA, Graham CH. Hypoxia induced resistance to doxorubicin in prostate cancer cells is inhibited by low concentrations of glyceryl trinitrate. J Urol 2003;170:1003–1007.

[9] Song X, Liu X, Chi W, Liu Y, Wei L, Wang X, Yu J. Hypoxia-induced resistance to cisplatin and doxorubicin in non-small cell lung cancer is inhibited by silencing of HIF-1a gene. Cancer Chemother Pharmacol 2006;58:776–784.

[10] Höckel M, Vaupel P. Tumor hypoxia: definitions and current clinical, biologic, and molecular aspects. J Natl Cancer Inst 2001;93:266–276.

[11] Wheeler RH, Dirks JW, Lunardi I, Nemiroff MJ. Effect of hyperbaric oxygen on the cytotoxicity of adriamycin and nitrogen mustard in cultured Burkitt's lymphoma cells. Cancer Res 1979;39:370–375.

[12] Kalns J, Krock L, Piepmeier EJ. The effect of hyperbaric oxygen on growth and chemosensitivity of metastatic prostate cancer. Anticancer Res 1998;18:363–368.

[13] Rharass T, Ribou AC, Vigo J, Salmon JM. Effect of adriamycin treatment on the lifetime of pyrene butyric acid in single living cells. Free Radic Res 2005;39:581–588.

[14] Rharass T, Vigo J, Salmon JM, Ribou AC. Variation of 1-pyrenebutyric acid fluorescence lifetime in single living cells with molecules increasing or decreasing reactive oxygen species levels. Anal Biochem 2006;357:1–8.

[15] Lautier D, Lahmy S, Canitrot Y, Vigo J, Viallet P, Salmon JM. Detection of human leukemia cells with multidrug resistant phenotype using multilabeling with fluorescent dyes. Anticancer Res 1993;13:1557–1564.

[16] Rocchi E, Vigo J, Viallet P, Bonnard I, Salmon JM. Multiwavelength videomicrofluorimetric study of cytotoxic effects of a marine peptide didemnin B on a normal and MDR resistant CCRF-CEM cell lines. Anticancer Res 2000;20:987–996.

[17] Savatier J, Vigo J, Salmon JM. Monitoring cell cycle distributions in living cells by videomicrofluorometry and discriminant factorial analysis. Cytometry A 2003;55A:8–14.

[18] Vigo J, Salmon JM, Lahmy S, Viallet P. Fluorescent image cytometry: from qualitative to quantitative measurements. Anal Cell Pathol 1991;3:145–165.

[19] Ribou AC, Vigo J, Salmon JM. Lifetime of fluorescent pyrene butyric acid probe in single living cells for measurement of oxygen fluctuation. Photochem Photobiol 2004;80:274–280.

[20] Nelder JA, Mead R. Numerical recipes; minimization or maximization of function. Comput J 1965;7:308–313.

[21] Stern O, Volmer M. The extinction period of fluorescence. Phys Z 1919;20:183–188.

[22] Zamzami N, Marchetti P, Castedo M, Zanin C, Vayssière JC, Petit PX, Kroemer G. Reduction in mitochondrial potential constitutes an early irreversible step of programmed lymphocyte death *in vivo*. J Exp Med 1995;181:1661–1672.

[23] Hagen TM, Yowe DL, Bartholomew JC, Wehr CM, Do KL, Park JY, Ames BN. Mitochondrial decay in hepatocytes from old rats: membrane potential declines, heterogeneity and oxidants increase. Proc Natl Acad Sci USA 1997;94:3064–3069.

[24] Robinson H, Gao YG, Bauer C, Roberts C, Switzer C, Wang A. H. 2′-deoxyisoguanosine adopts more than one tautomer to form base pairs with thymidine observed by high-resolution crystal structure analysis. Biochemistry 1998;37:10897–10905.

[25] Fossati G, Moulding DA, Spiller DG, Moots RJ, White MRH, Edwards SW. The mitochondrial network of human neutrophils: role in chemotaxis, phagocytosis, respiratory burst activation, and commitment to apoptosis. J Immunol 2003;170:1964–1972.

[26] Robertson JD, Orrenius S, Zhivotovsky B. Nuclear events in apoptosis. J Struct Biol 2000;129:346–358.

[27] Proskuryakov SY, Konoplyannikov AG, Gabai VL. Necrosis: a specific form of programmed cell death? Exp Cell Res 2003;283:1–16.

[28] Duranteau J, Chandel NS, Kulisz A, Shao Z, Schumacker PT. Intracellular signaling by reactive oxygen species during hypoxia in cardiomyocytes. J Biol Chem 1998;273:11619–11624.

[29] Guzy RD, Hoyos B, Robin E, Chen H, Liu L, Mansfield KD, Simon MC, Hammerling U, Schumacker PT. Mitochondrial complex III is required for hypoxia-induced ROS production and cellular oxygen sensing. Cell Metab 2005;1:401–408.

[30] Vaux EC, Metzen E, Yeates KM, Ratcliffe PJ. Regulation of hypoxia-inducible factor is preserved in the absence of a

functioning mitochondrial respiratory chain. Blood 2001;98:296–302.

[31] Michelakis ED, Thebaud B, Weir EK, Archer SL. Hypoxic pulmonary vasoconstriction: redox regulation of O_2-sensitive K^+ channels by a mitochondrial O_2-sensor in resistance artery smooth muscle cells. J Mol Cell Cardiol 2004;37:1119–1136.

[32] Göhde W, Meistrich M, Meyn R, Schumann J, Johnston D, Barlogie B. Cell-cycle phase-dependence of drug-induced cycle progression delay. J Histochem Cytochem 1979;27:470–473.

[33] Traganos F, Israel M, Silber R, Seshadri R, Kirschenbaum S, Potmesil M. Effects of new N-alkyl analogues of adriamycin on *in vitro* survival and cell cycle progression of L1210 cells. Cancer Res 1985;45:6273–6279.

[34] Gebhardt MC, Kusuzaki K, Mankin HJ, Springfield DS. An assay to measure adriamycin binding in osteosarcoma cells. J Orthop Res 1994;12:621–627.

[35] Swift LP, Rephaeli A, Nudelman A, Phillips DR, Cutts SM. Doxorubicin-DNA adducts induce a non-topoisomerase II-mediated form of cell death. Cancer Res 2006;66:4863–4871.

[36] Skladanowski A, Konopa J. Adriamycin and daunomycin induce programmed cell death (apoptosis) in tumour cells. Biochem Pharmacol 1993;46:375–382.

[37] Ling YH, Priebe W, Perez-Soler R. Apoptosis induced by anthracycline antibiotics in P388 parent and multidrug-resistant cells. Cancer Res 1993;53:1845–1852.

[38] Müller I, Jenner A, Bruchell G, Niethammer D, Halliwell B. Effect of concentration on the cytotoxic mechanism of doxorubicin—apoptosis and oxidative DNA damage. Biochem Biophys Res Commun 1997;230:254–257.

[39] Hockenbery DM, Oltvai ZN, Yin XM, Milliman CL, Korsmeyer SJ. Bcl-2 functions in an antioxidant pathway to prevent apoptosis. Cell 1993;75:241–251.

[40] Slater AFG, Nobel CSI, Orrenius S. The role of intracellular oxidants in apoptosis. Biochim Biophys Acta 1995;1271:59–62.